Journal of Virological Methods 326 (2024) 114907

Contents lists available at ScienceDirect

Journal of Virological Methods

journal homepage: www.elsevier.com/locate/jviromet

Protocols

An optimised protocol for the expression and purification of adenovirus core protein VII

Ajani Athukorala [a], Karla J. Helbig [a], Brian P. McSharry [b], Jade K. Forwood [b], Subir Sarker [c,*]

[a] Department of Microbiology, Anatomy, Physiology, and Pharmacology, School of Agriculture, Biomedicine and Environment, La Trobe University, Melbourne, VIC 3086, Australia
[b] School of Dentistry and Medical Sciences Biomedical Sciences, Charles Sturt University, Wagga Wagga, New South Wales, Australia
[c] Biomedical Sciences and Molecular Biology, College of Public Health, Medical and Veterinary Sciences, James Cook University, Townsville, QLD 4811, Australia

ARTICLE INFO

Keywords:
Adenovirus core protein
Core protein VII purification
DNA binding protein
RNase
pVII

ABSTRACT

Adenovirus protein VII (pVII) is a highly basic core protein, bearing resemblance to mammalian histones. Despite its diverse functions, a comprehensive understanding of its structural intricacies and the mechanisms underlying its functions remain elusive, primarily due to the complexity of producing a good amount of soluble pVII. This study aimed to optimise the expression and purification of recombinant pVII from four different adenoviruses with a simple vector construct. This study successfully determined the optimal conditions for efficiently purifying pVII across four adenovirus species, revealing the differential preference for bacterial expression systems. The One Shot BL21 Star (DE3) proved favourable over Rosetta 2 (DE3) pLysS with consistent levels of expression between IPTG-induced and auto-induction. We demonstrated that combining chemical and mechanical cell lysis is possible and highly effective. Other noteworthy benefits were observed in using RNase during sample processing. The addition of RNase has significantly improved the quality and quantity of the purified protein as confirmed by chromatographic and western blot analyses. These findings established a solid groundwork for pVII purification methodologies and carry the significant potential to assist in unveiling the core structure of pVII, its arrangement within the core, DNA condensation intricacies, and potential pathways for nuclear transport.

1. Introduction

Adenoviruses (AdVs) are nonenveloped viruses that contain double-stranded DNA genomes that can infect humans and animals (Benkő et al., 2021; Harrach et al., 2022; Maclachlan and Dubovi, 2017; Medkour et al., 2020). In humans, adenoviruses typically do not cause severe illness in individuals with a healthy immune system, but they can lead to more serious infections in individuals with weakened immune systems (Chen and Tian, 2018; Lynch and Kajon, 2016). Conversely, many adenoviruses infecting animals have been linked to causing significant health issues with varying clinical outcomes depending on the host species (Harrach et al., 2019; Karamendin et al., 2021; Needle et al., 2019; Syamily et al., 2022).

Adenovirus virions have complex protein structures consisting of capsids, surrounding their DNA genome and core proteins. The three primary capsid proteins are hexon, penton base, and fiber (Gallardo et al., 2021; Kulanayake and Tikoo, 2021; San Martín, 2012), and four cement (minor capsid) proteins, are IIIa, VI, VIII, and IX. Alongside these capsid proteins, the adenovirus core structure consists of a range of other core proteins, such as three prominent, and highly basic proteins: V, VII, X (μ), a non-basic terminal protein, IVa2, and adenovirus encoded protease (Gallardo et al., 2021; Kulanayake and Tikoo, 2021; Nemerow et al., 2012). These core proteins play essential roles in various stages of the viral life cycle. Protein V mainly contributes to the assembly of the viral particle and is only present in mastadenoviruses (Pérez-Vargas et al., 2014; Ugai et al., 2007). Protein X is involved in packaging and condensing the viral genome (Kulanayake and Tikoo, 2021) while terminal protein (pTP) contributes to the initiation of DNA replication (Mysiak et al., 2004).

Protein VII, exists in approximately 800 copies per virion (Gallardo et al., 2021; Ostapchuk et al., 2017) and is the most abundant core protein in adenovirus, serving a multifunctional role in the viral lifecycle (Gallardo et al., 2021). Notably, adenoviral pVII is implicated in the facilitation of transcription for early genes, genome condensation, and acts as a powerful transcription repressor following nuclear entry (Johnson et al., 2004). By interacting with viral DNA, it aids in

* Corresponding author.
E-mail address: subir.sarker@jcu.edu.au (S. Sarker).

https://doi.org/10.1016/j.jviromet.2024.114907
Received 5 November 2023; Received in revised form 25 February 2024; Accepted 26 February 2024
Available online 2 March 2024

Table 1
Protein sequences of the chosen adenoviruses in this study.

Adenovirus	Protein Size (aa)	pVIII MW (kDa)	Recombinant pVII MW (kDa)	Isoelectric point (pH)	Sequence
Passerine atadenovirus 1 (PaAdV pVII)	115	13.02	14.69	12.39	MALISPSDNTGWGALGRSALRATGASFSVRQPVRVRAHYRSQWGQ RNGRIGYRTLRKNLQAYVRRHYSTVRRRKRPASGVLVGVSTAKSAF GARVAARAVRSILNARRRRRRARR
Psittacine siadenovirus F (PsSiAdV pVII)	129	13.9	15.57	11.75	MTTYLYSPADNRGWGLGESTMRDYYLIGGALQPSDVYTVRVREHWR RKRGTARPRAVVASVAPVVPAVTVRRARKRAIAIPTTRLLRSATRAAA PAVPVAPGALVPAVAPAPAVPFVASPGGFKRRRLT
Frog siadenovirus A (FAdV pVII)	149	15.99	17.66	11.82	MTAVLLSPADNRGWGARAMRGSGVYLVGGASAPSDVYTEHVRGYWR RKRSKKAVATTTVTPVVGAVGPLWTGSRKKIPKTPVGVVGPLWQGTRK RGTRVLGPLGPSWQPWGRKIKKARAPVIPMDITPVVDAAGPVVVSV PPRKRRRVA
Human mastadenovirus C (HAdV pVII)	198	21.9	23.9	12.19	MSILISPSNNTGWGLRFPSKMFGGAKKRSDQHPVRVRGHYRAPWGAHK RGRTGRTTVDDAIDAVVEEARNYTPTPPPVSTVDAAIQTVVRGARRYAK MKRRRRRVARRHRRRPGTAAQRAAAALLNRARRTGRRAAMRAARRLA AGIVTVPPRSRRRAAAAAAAAISAMTQGRRGNVYWVRDSVSGLRVPVRTRPPRN

Note. aa-amino acids

compacting the viral genome within the capsid (Dai et al., 2017; Kulanayake and Tikoo, 2021; Zhang and Arcos, 2005). The positively charged amino acid residues, especially arginine, in protein VII contribute to its histone-like DNA binding properties, owing to its highly basic nature (Prage and Pettersson, 1971; Sharma et al., 2017). Moreover, research by Ostapchuk et al. (2017), Karen and Hearing (2011) and Xue et al. (2005) highlights the ongoing roles of pVII during adenovirus maturation and DNA replication in the early stages of viral infection. Additionally, several functional analyses have demonstrated the role of pVII for genome nuclear import (Davison et al., 2000; Hindley et al., 2007; Lee et al., 2003; Wodrich et al., 2006). However, the mechanisms governing these functions have remained elusive or subject to conflicting ideas partly due to the lack of structural information. Apart from the recent cryo-EM structure analysis that revealed the binding of the cleaved N-terminus of precursor protein VII with hexon in human adenovirus 5 (Dai et al., 2017), the pVII structure has not been defined. Additionally, cryo-EM is generally less effective for analysing small proteins and may have resolution limitations (Benjin and Ling, 2020). Therefore, pVII purification will be beneficial for further characterisation, but limited information is available.

On the other hand, previous studies on pVII protein sequences from different species (Athukorala et al., 2024; Hindley et al., 2007; Wodrich et al., 2006) and unpublished data have demonstrated significantly diverse behaviours in nuclear import. Therefore, studying pVII purification, particularly pVII from different species, will be important. In this study, we sought to express and purify adenovirus pVII of four adenoviruses using bacterial expression systems. We have experimented with standard protein purification techniques and protein recovery from inclusion bodies (Haruki et al., 2003; Singh et al., 2015) to achieve higher concentrations of purified pVII. In this report, we present an optimised protocol for the expression and purification of protein VII, utilizing pVII sequences from four distinct adenovirus species: *Human mastadenovirus C* (Kovács et al., 2004), *Frog siadenovirus A* (Davison et al., 2000), psittacine siadenovirus F (Athukorala et al., 2020; Athukorala et al., 2021), and passerine adenovirus 1 (Athukorala et al., 2020), representing three major genera in the family.

2. Materials and Methods

2.1. Construct design and synthesis

Protein VII sequences from adenoviruses were obtained from GenBank and utilised to create expression vector constructs with pET30a+. Four distinct adenovirus species, namely psittacine siadenovirus F (PsSiAdV) (GenBank accession no. MW365934) (Athukorala et al., 2021), passerine adenovirus 1 (PaAdV) (GenBank accession no. MT674683) (Athukorala et al., 2020), frog siadenovirus A (FAdV) (GenBank accession no. NC_002501) (Davison et al., 2000), and human mastadenovirus C (HAdV) (GenBank accession no. AC_000017) (Kovács et al., 2004) were chosen for this study and are detailed in Table 1. The constructs were synthesised by GenScript (GenScript Biotech, New Jersey), with a schematic representation of the VII-pET30a(+) expression vector incorporated with the 6xHis tag and the TEV cleavage site N-terminal to protein VII (Supplementary Figure S1). Comparisons of pVII sequences across above mentioned four species, demonstrating similarities are provided in Supplementary Figure S2.

2.2. Expression of recombinant protein VII

In the preliminary analysis, three different *E. coli* cell lines; Rosetta 2 (DE3) Singles, Rosetta 2(DE3) pLysS Singles, and One Shot BL21 Star (DE3) and two distinct expression systems were assessed to determine the optimal workflow. The plasmids were transformed into chemically competent *E. coli* cells by the heat shock (42^0 C for 45 s) method. After transformation, the cells were plated on a selective LB medium supplemented with kanamycin and incubated overnight to isolate the transformed colonies. The compositions of used mediums, buffers and reagents are given in the Supplementary Table S1.

Starter cultures were prepared by inoculating a single colony into falcon tubes containing 5 mL of LB broth and 50 µg/mL kanamycin. These cultures were then incubated overnight at 37°C in a shaking incubator at 225 rpm. For bulk expression, 5 mL of the starter culture was added to 960 mL of sterilised expression media in a baffled flask containing 50 µg/mL kanamycin. In the case of auto-induction trials, the media was supplemented with NPS, 5052 (Supplementary Table S1), and $MgCl_2$ to reach a total volume of 1 L of culture. The flask was incubated at room temperature for 24 h in a shaker set at 110 rpm. For IPTG-induced expression, 60 mL of NaCl was added to bring the total volume to 1 L, and the culture was propagated at 37°C until reaching an OD600 of 0.6 (Nanophotometer, Implen). Then, IPTG (1 mM) was added to induce expression, and the culture was incubated overnight at room temperature in a shaker.

Following incubation, the cells were harvested by centrifugation at 6000 rpm for 30 min at 4°C using a HITACHI CR22N centrifuge. The cell pellet was resuspended in 15 mL of HIS A buffer (Supplementary Table S1) and stored at −20°C in a falcon tube until further purification.

2.3. Lysis of E. coli cells

In the preliminary analysis, three different methods; freeze/thaw method of mechanical cell lysis, chemical cell lysis using FastBreak cell lysis reagent (Promega), and cell lysis by sonication have been tested, and a combination of these methods were utilised to extract protein VII. Harvested bacterial cell pellets were subjected to two freeze/thaw cycles

by thawing in cold water and freezing again at −20°C. Chemical lysis of thawed cell pellets was performed by treating with 10 µl of DNase (50 µg/mL) to clear the cellular DNA, 10 µl of RNase (50 µg/mL) and 1 mL of lysozyme for 20 mL of culture followed by incubation on ice for 1 h with frequent vigorous mixing. Experiments were conducted with and without FastBreak to determine the effectiveness. To ensure thorough cell lysis, the cell suspension was subjected to three rounds of sonication (Branson sonifier 250), each lasting 30 seconds at an output of 30 watts, and cooling on ice between each sonication cycle. The resulting cell lysate was then centrifuged at 13,000 rpm for 30 min at 4°C using HITACHI CR22N centrifuge.

For the pVII analysis, both the soluble and insoluble fractions were extracted and purified. In the case of the soluble fraction, the supernatant was filtered through a 0.45 µm MF- Millipore MCE membrane syringe filter (MILLEX HA) to remove any insoluble particles prior to being loaded onto affinity column (His tag protein purification columns) for protein purification. To isolate protein VII in the insoluble fraction, a protocol incorporating a denaturing step was followed as explained in the Section 2.5.

2.4. Purification of protein VII – from the soluble fraction

Vector constructs used in this study were designed to incorporate 6xHIS tag and therefore pVII proteins with His-tags were purified using nickel-affinity columns employing an AKTA Pure Scientific FPLC (Cytiva). For the purification, protein samples were loaded onto 5 mL His-Trap HP His tag protein purification columns (Cytiva) on FPLC that had been pre-equilibrated with His buffer A. Subsequently, washes with 15 column volumes of His buffer A were performed to remove any unbound protein. the bound proteins were then eluted using an increasing gradient of His buffer B, which contained a higher concentration of imidazole (Supplementary Table S1). During elution, fractions were collected based on the observed peaks in the chromatogram and treated with TEV protease enzyme overnight at 4^0 C to remove 6xHis tag before size exclusion chromatography.

2.5. Purification of protein VII – from the insoluble fraction

The insoluble cell lysate was resuspended in a denaturing buffer containing 8 M urea, which served as the denaturing agent and incubated on ice for 30 min. The supernatant was collected by centrifugation at 13,000 rpm for 30 min at 4°C in HITACHI CR22N centrifuge and filtered through 0.45 µm filter. For protein extraction, the His-tag Ni-NTA purification method was employed, utilising gravitational force. The Gravity flow column used for purification was setup and added the HisPur Ni-NTA resin (Thermo Fisher Scientific). Resin was pre-equilibrated with the denaturing buffer (Supplementary Table S2) following the manufacturers protocol, prior to passing the protein extract through the column. To eliminate unbound proteins, the column was washed with 5 column volumes of washing buffer (Supplementary Table S2) before the bound proteins were eluted using an elution buffer containing 100 mM imidazole. A schematic illustration detailing the major steps is given in Fig. 1.

The fractions obtained through affinity purification were pooled together and dialysed using 7 K molecular weight cut-off SnakeSkin Dialysis Tubing (Thermo Fisher Scientific) overnight at 4°C to remove the denaturing agent, urea. Two commonly used buffers, Tris (pH 8) and GST A (pH 8) were tested to identify the suitable buffer condition for the dialysis. Dialysed sample was centrifuged at 3000 rpm for 2 min to spin down the precipitated protein and the soluble fraction was concentrated

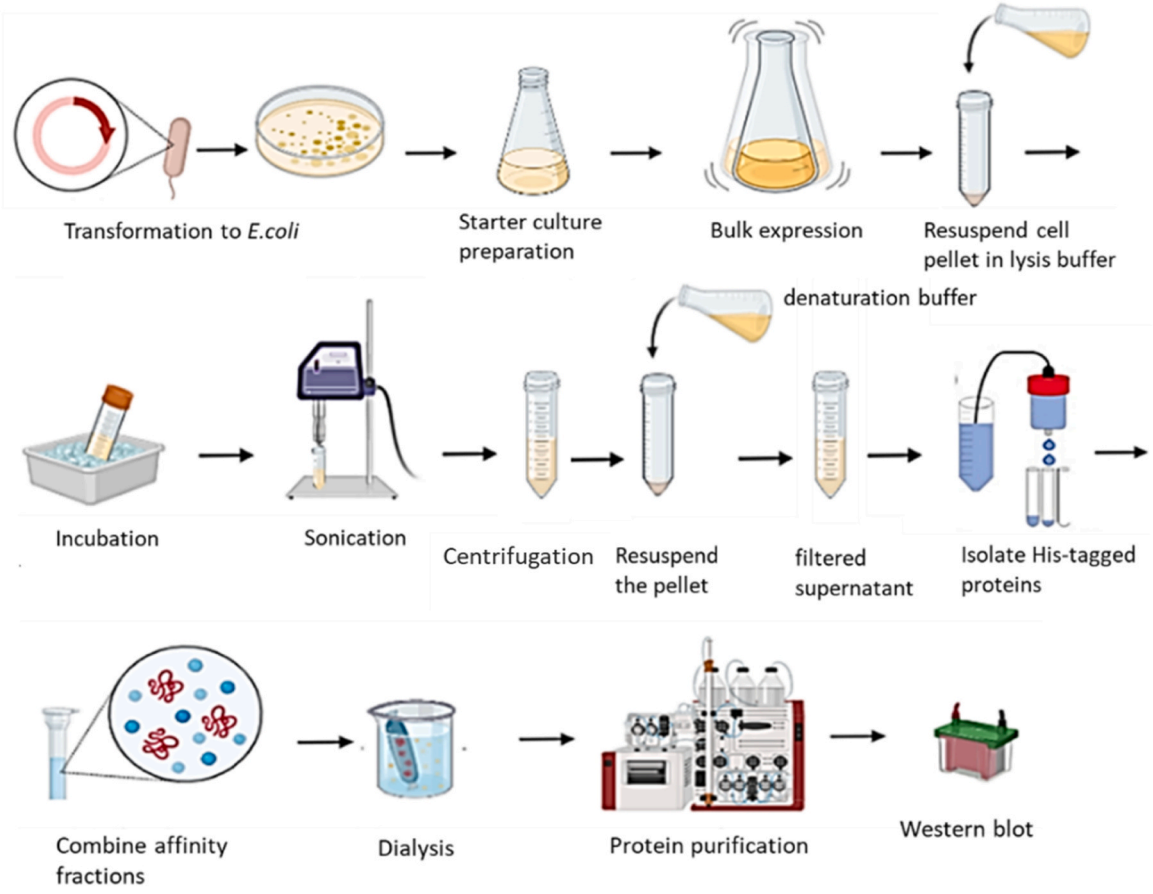

Fig. 1. Diagrammatic representation of major steps involved in protein purification of insoluble proteins employed in this study. The figure was generated using BioRender.

by reducing to a final volume of 500 µl using a 10kD MWCO Amicon Ultra-15 centrifugal filter unit (Merck Millipore, Burlington, MA, USA). In order to determine the native molecular weight of proteins, the concentrated protein sample was injected into AKTA pure FPLC machine for analytical size exclusion chromatography. The procedure was performed similarly to preparative size exclusion chromatography, utilising an analytical Superdex 200 small scale SEC column with a maximum injection volume of up to 500 µLs. Fractions corresponding to the peak observed were collected and subsequently visualised using western blot.

2.6. Protein VII visualisation

2.6.1. SDS-PAGE

SDS-PAGE (Thermo Fisher Scientific) was utilised as a visual tool to observe protein samples collected at various steps to assess the efficacy of expression and purification processes. Fractions collected for SDS analysis during protein purification are listed in Supplementary Table S2.

2.6.2. Western blot

Samples collected at different steps of the protein VII purification were combined with 2x loading buffer (Novex Tris-Glycine SDS Sample Buffer (2X), Invitrogen, Thermo Fisher Scientific) and heated to 95°C for 5 min in a heat block. Protein samples were loaded into 10-well, 4–15% Mini-PROTEAN TGX stain-free gel (BioRad) alongside 5 µl of Precision Plus Standards-Kaleidoscope (BioRad). Gel was run at 160 V for 30 min in a running buffer (Supplementary Table S1). Gel was visualised under the Bio-Rad Gel Doc EZ Imager to assure the presence of proteins prior to transfer. Activated nitrocellulose membrane with methanol, SDS gel, and filter papers/pads were wet in the transfer buffer (Supplementary Table S1) and assembled as per the manufacturer's direction. Proteins were transferred onto Nitrocellulose Blotting Membranes (BioRad) in cold transfer buffer (Supplementary Table S1) using a NICE Thermo Fisher Scientific, Invitrogen Mini Trans Blot at 10 V for 1 h.

Following the transfer, the nitrocellulose membrane was washed in TBS (Table 1) for 5 min. 1% casein in TBS was used as the blocking buffer and the membrane was incubated for 1 h at room temperature in a shaker set to 50 rpm. Diluted mouse anti-Histadine tag:DyLight antibody (BioRad) in blocking buffer at 1:1000 was added to the membrane and incubated overnight at 4^0 C in a laboratory rotor. The incubated membrane was then washed three times with 10 min interval and imaged.

3. Results

3.1. Selection of an expression system and lysis condition

Individual proteins prefer different bacterial cell lines and expression conditions. Therefore, as a preliminary analysis, the obtained vector constructs were expressed in different *E. coli* cell lines using two different expression systems. Plasmid constructs were transformed into chemically competent *E. coli* cells and transformed colonies were identified and expressed. The isolated soluble cell lysate was visualised by SDS-PAGE (Fig. 2). Initially, all constructs were expressed in One Shot BL21 Star (DE3) and PsSiAdV and FAdV constructs were observed to express well in One Shot BL21 Star (DE3) under both auto and IPTG-induced expression conditions (Fig. 2**A**). Poorly expressed PaAdV and HAdV were then introduced to Rosetta 2 (DE3) pLysS and Rosetta 2 (DE3) *E. coli* cell lines and both preferred Rosetta 2 (DE3) pLysS (Fig. 2**B**). IPTG-induced and auto-induction resulted in comparatively similar expression (Fig. 2**B**), but the IPTG-induced expression system was selected and used for all four constructs.

Following the initial analysis, we initiated the large-scale expression of pVII protein (6 L) utilising PsSiAdV and FAdV constructs. One Shot BL21 Star (DE3) cells were transformed with the plasmid constructs and induced with IPTG to express the proteins. After purification through affinity and size exclusion techniques, the protein profiles were assessed using SDS-PAGE. Fig. 3**A** and **B** illustrate the SDS gel images and SE chromatograms for PsSiAdV and FAdV pVII, respectively.

The SDS gels revealed the presence of protein bands in the soluble cell lysate and purified affinity fractions, with the expected sizes of 14 kDa for PsSiAdV and 17 kDa for FAdV. Notably, in the PsSiAdV purification, a distinct protein band appeared slightly above the 14 kDa mark, corresponding to the elution of PsSiAdV pVII at peak 2 in the chromatogram. However, the elution of FAdV pVII at peak 1 is questionable due to the wide and overlapping peaks observed in the chromatogram. Although the SDS gels displayed reasonably intense bands, the protein concentrations were insufficient for further analysis.

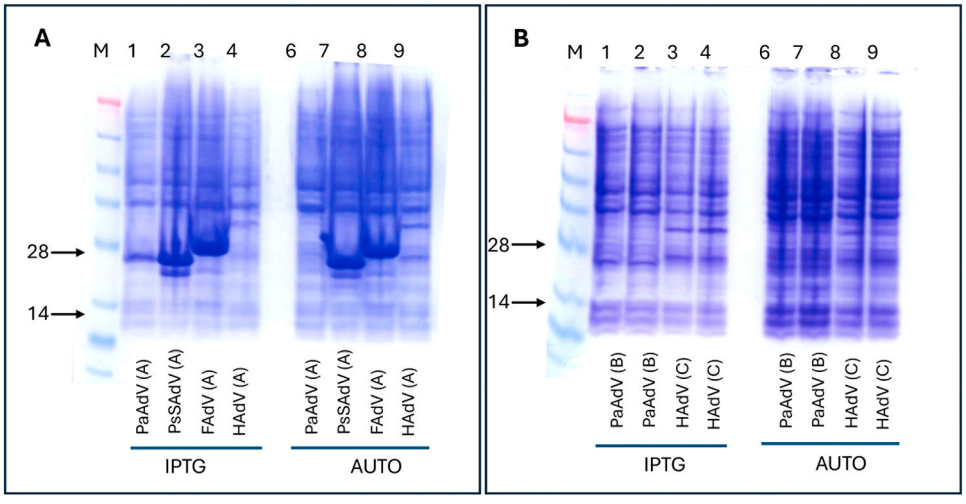

Fig. 2. Preliminary analysis for *E. coli* cell line and expression system selection (**A**) SDS-PAGE gel electrophoresis showing AUTO and IPTG induced expression of pVII from PaAdV, PsSAdV, FAdV and HAdV. Lane M is a molecular weight marker (SeeBlue Plus2 protein standard, Thermo Fisher Scientific). Lane 1–4 for IPTG induced expression and 6–9 for AUTO induction. Lanes 1–4 and 6–9 were loaded with bacterial cell pellets from PaAdV, PsSAdV, FAdV, and HAdV pVII expression, respectively. (**B**) SDS-PAGE gel electrophoresis showing AUTO and IPTG induced expression of pVII from PaAdV, and HAdV in Rosetta 2(DE3) pLysS and Rosetta 2 (DE3) *E. coli* cell lines. Lane M is a molecular weight marker (SeeBlue Plus2 protein standard, Thermo Fisher Scientific). Lane 1–4 for IPTG induce expression and 6–9 for AUTO induction. Lanes 1, 2, 6, and 7 for PaAdV pVII expression and lanes 3,4, 8, and 9 for HAdV pVII expression. The *E. coli* cell lines utilised for expressing proteins, namely One Shot BL21 Star (DE3), Rosetta 2(DE3) pLysS, and Rosetta 2 (DE3), were designated as A, B, and C in parentheses, respectively.

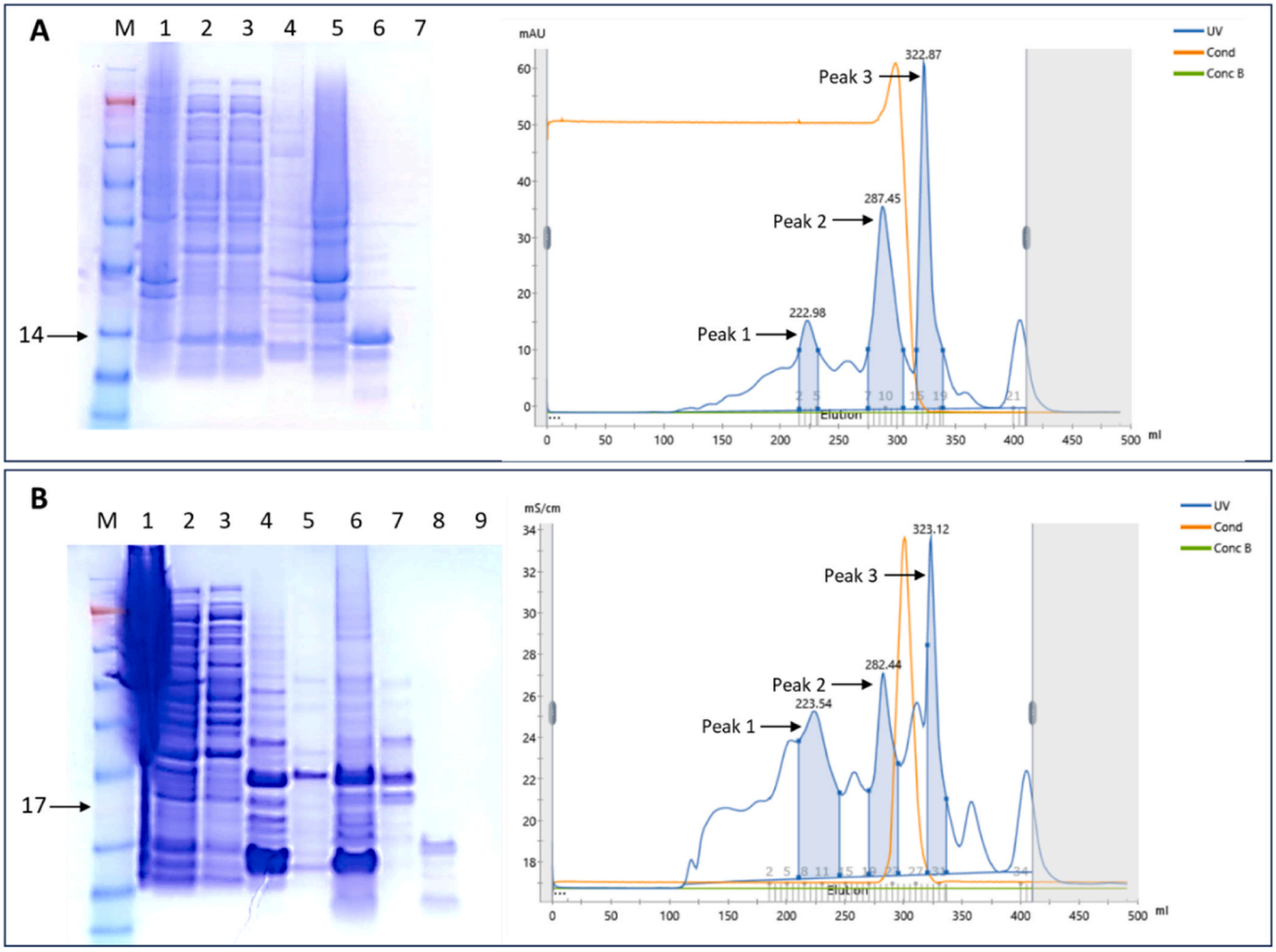

Fig. 3. SDS-PAGE gel visualising the steps of PsSiAdV pVII and FAdV pVII expression in One Shot BL21 Star (DE3) *E. coli*. (**A**) protein profiles at different stages of PsSiAdV pVII purification were visualised on the SDS-PAGE gel: Lane M; molecular weight marker (SeeBlue Plus2 protein standard, Thermo Fisher Scientific), Lane 1;bacterial cell pellet, Lane 2; soluble cell extract, Lane 3; flowthrough from affinity purification, Lane 4; pooled affinity purified factions, Lane 5; SEC fraction for peak 1, Lane 6; SEC fraction for peak 2, and Lane 7; SEC fraction for peak 3. The right panel shows the SE chromatogram of PsSiAdV pVII, resulting three significant peaks for the pooled affinity purified protein sample. (**B**) Protein profiles at different stages of FAdV pVII purification: Lane M; the molecular weight marker (SeeBlue Plus2 protein standard, Thermo Fisher Scientific), Lane 1; bacterial cell pellet, Lane 2; soluble cell extract, Lane 3; flowthrough from affinity purification, Lane 4; affinity fraction 1, Lane 5; affinity fraction 2, Lane 6; pooled affinity purified factions, Lane 7; SEC fraction for peak 1, Lane 8; SEC fraction for peak 2, and Lane 9; SEC fraction for peak 3. The right panel shows the SE chromatogram of FAdV pVII, resulting three significant peaks for the pooled affinity purified protein sample.

Protein VII is classified as a highly basic protein that functions as a DNA-binding protein. It is plausible that pVII might also interact with RNA, which could contribute to the wide peaks observed in the chromatogram. To enhance the purification process and obtain purer proteins, we conducted experiments involving three distinct cell lysis approaches including RNase treatment.

To evaluate the effect of RNase treatment on the purification outcome, FAdV pVII was expressed and tested. The FAdV pVII cell pellet was divided into two halves. RNase was added to one half during cell lysate processing, while the other half was treated with RNase after affinity purification. By comparing the expression profiles under two different conditions, as depicted in Fig. 4**A**, it was observed that the addition of RNase after affinity purification had a significant impact. Specifically, it resulted in a reduction of the wide, overlapping peaks, leading to the emergence of a single significant peak.

To facilitate cell lysis, the extracted cells underwent two freeze/thaw cycles. Lysozyme was then added to disrupt the cell walls, while DNase and RNase were employed to denature associated nucleotides. In order to optimize the cell lysis process, these steps were further refined using three different methods. The extracted cell pellets from FAdV pVII expression were subjected to chemical cell lysis with and without the addition of FastBreak and through sonication. When comparing the results of each method, it was observed that chemical cell lysis yielded similar purification profiles, indicating a likely consistency in protein content. However, mechanical cell lysis by sonication resulted in a slightly low protein profile (Fig. 4**B**). Based on these findings, a hybrid approach was adopted, which involved two freeze/thaw cycles, followed by chemical cell lysis and sonication, to extract protein VII.

3.2. *Method optimisation for the purification of insoluble pVII*

Higher protein concentrations are essential for downstream applications including structural analysis. However, the soluble fraction of the expressed proteins showed faint protein bands and yielded notably low protein concentrations when visualised on SDS gels. Thus, the method was revised to include steps commonly employed in the purification of inclusion bodies in order to isolate the insoluble pVII.

pVII was affinity purified under denaturing conditions and eluted

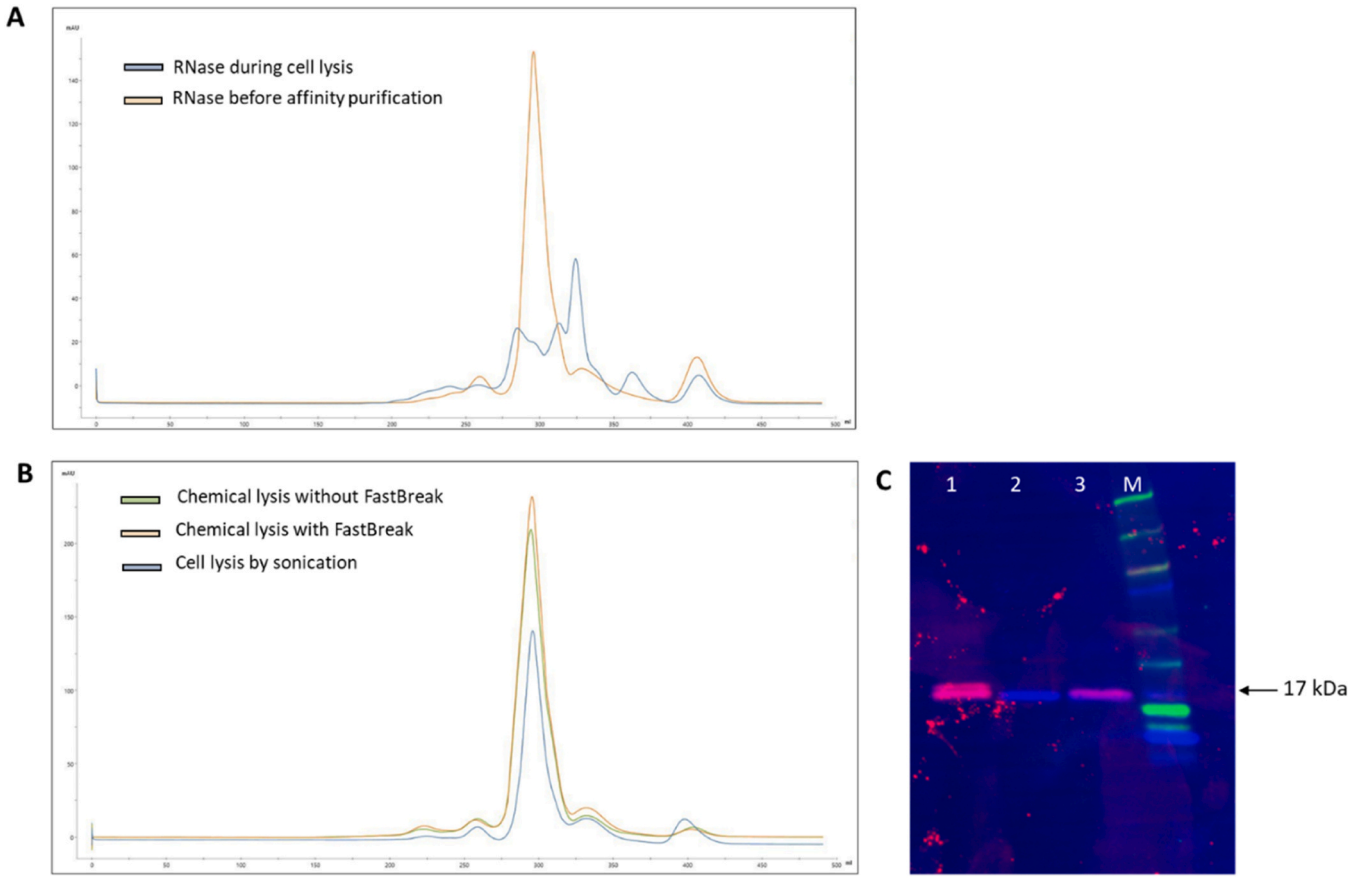

Fig. 4. The FPLC chromatograms to provide an overview of the purification profile for FAdV pVII expression under different cell lysis conditions. (**A**) A comparison of FAdV pVII purification profiles showing the impact of RNase treatment at two different stages of the purification process. The orange line represents the chromatogram when RNase was added to the soluble cell extract prior to affinity purification which resulted in a single significant peak, indicating an improved purification outcome. Instead, the chromatogram for RNase treatment during cell lysis (blue line) did not exhibit a clear effect on the purification profile. (**B**) The chromatogram demonstrates the effects of employing FastBreak or sonication during cell lysis. A bacterial cell pellet obtained from FAdV pVII expression was divided into three portions and treated differently during cell lysis: one portion using the standard method without FastBreak, another portion with additional cell lysis using FastBreak solution, and the third portion through sonication. The results showcased a positive outcome, indicating enhanced cell lysis and protein collection when FastBreak was utilised (orange line) in comparison to the previously employed standard method (green line) and sonication (blue line). (**C**) Western blot analysis visualising the protein fractions collected at the highest peak corresponding to the size exclusion chromatogram. Lanes 1, 2, and 3 present proteins purified following cell lysis without FastBreak, with FastBreak solution, and through sonication, respectively. Lane M presents the 250 kDa molecular ladder.

with high imidazole concentration. His tagged target pVII was detected in western blot using mouse anti-his-tag antibodies resulting in intense protein bands at the expected size range. The analysis based on HAdV is presented in Fig. 5. Eluted affinity fractions were pooled and dialysed overnight at 4°C to prevent protein degradation. A significant amount of protein was precipitated after the dialysis (Fig. 5**A**) and couldn't be used for further purifications via SEC. Therefore, the soluble fraction was collected and analytically purified. Interestingly, considerably higher concentrations of HAdV pVII resulted after the FPLC purification (Fig. 5**A** and **B**) indicating the potential use of soluble protein fraction after dialysis and purification, for downstream applications.

Dialysis was carried out using two commonly used buffers, GST A buffer (pH 8), and tris buffer (pH 8). The FPLC chromatogram (Fig. 5**B**) and western blot analysis (Fig. 5**C**) indicated that either buffer condition could be employed effectively. Here, the protein sample dialysed with Tris buffer was concentrated to one-third of the volume compared to the sample treated with GST A buffer prior to injection into FPLC purification system. This difference in concentration accounted for the observed variation in the UV absorbance, giving a reading of 1200 mAU for the Tris buffer sample and 400 mAU for the GST A buffer sample at the highest peak in the chromatogram. Similarly, the intensity of the protein band in the western blot (Fig. 5**C**) is concentration dependent.

4. Discussion

Adenovirus pVII is an essential protein found in the core of the adenovirus virion with crucial roles in genome packaging, virion assembly, and stabilising the viral capsid during maturation and infection (Avgousti et al., 2017; Gallardo et al., 2021; Kulanayake and Tikoo, 2021; Lee et al., 2003). However, comprehensive insights into its precise functions and structural intricacies remain elusive due to the limited research on purifying recombinant proteins VII (Dai et al., 2017; Sharma et al., 2017). By refining these methodologies, our aim was to provide an optimised protein production workflow for adenovirus pVII proteins to facilitate their further structural and functional understanding. This report highlights the promising results achieved by employing a combination of lysis techniques with incorporation of RNase treatment to enhance protein purification. Our approach also exhibited the capability to extract pVII in the soluble fraction, despite its tendency towards precipitation. These advancements will enable a deeper exploration of the protein's functional dynamics, contributing significantly to our understanding of adenovirus biology.

The present investigation commenced by focusing on four distinct adenovirus species, representing three diverse genera within the family. The rationale underpinning the choice of PaAdV and FAdV was their representation of ancient nodes within the phylogenetic trees of the

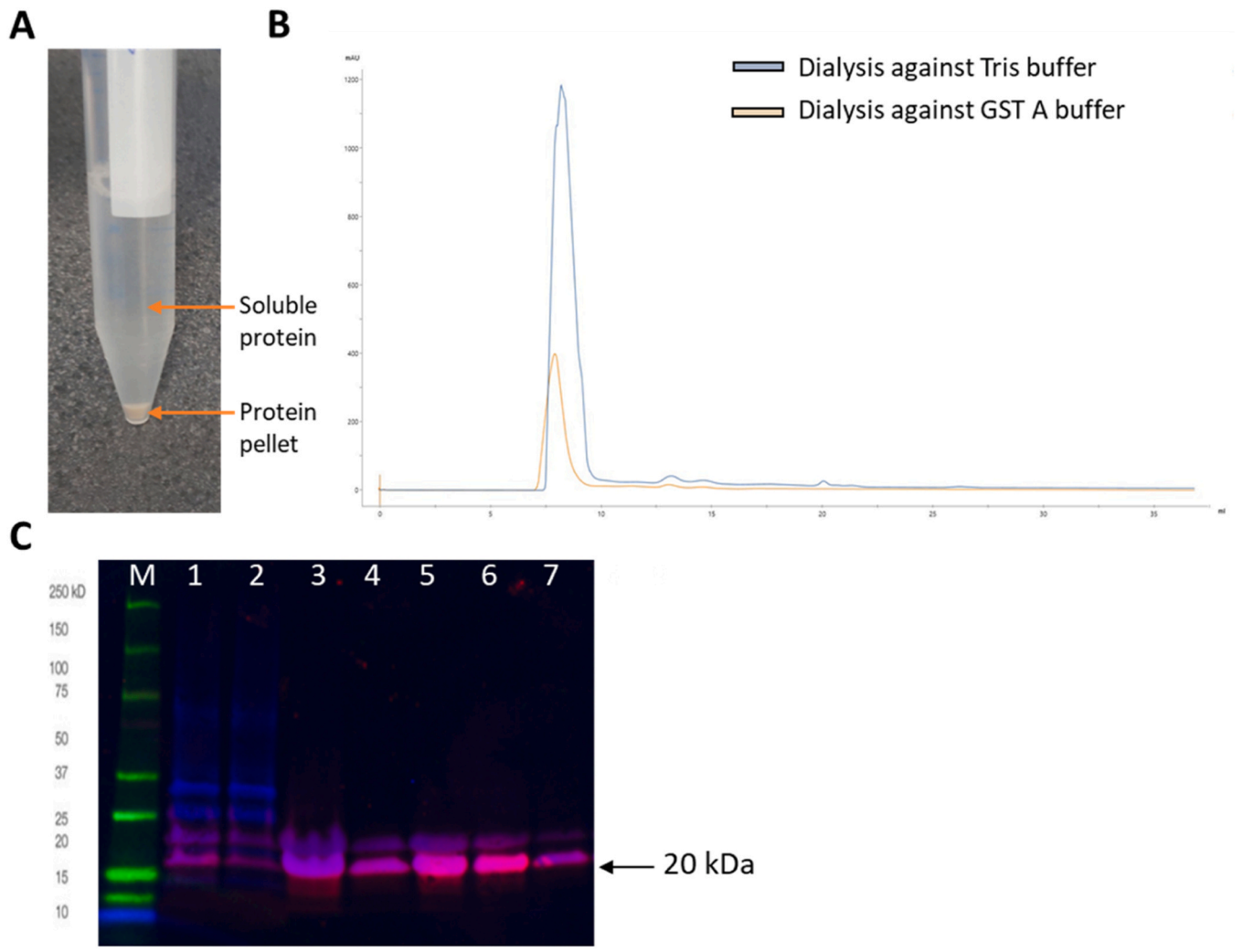

Fig. 5. Purification and characterisation of insoluble HAdV pVII under denaturing conditions. (**A**) Image displaying the precipitated HAdV protein following affinity purification and dialysis. The protein pellet and liquid fractions are indicated by arrows. (**B**) Chromatogram illustrating the analytical purification profile of HAdV pVII, showing a significant single peak indicating a higher protein content in the sample. The dialysed proteins against Tris buffer (blue line) and GST A buffer (orange line) are depicted in the chromatogram. The sample dialysed with Tris buffer was three times more concentrated than the other sample and therefore either buffer can be used for the dialysis. (**C**) Western blot analysis visualising the protein collected at different stages of the purification process. The presence of His-tagged HAdV pVII is indicated by the pink colour in the western blot. The molecular weight marker (Precision Plus Protein Kaleidoscope Pre-stained Protein Standard) in lane M; supernatant collected after denaturation with urea in lane 1; flowthrough and a fraction from affinity purification in lane 2 and 3; soluble fraction after dialysis with Tris buffer in lane 4; fraction corresponding to peak 1 in lane 5, soluble fraction after dialysis with GST A buffer lane 6; fraction representing peak 2 in the chromatogram for the protein sample dialysed with GST A buffer in lane 7.

Atadenovirus and *Siadenovirus* genera, respectively (Athukorala et al., 2022). The recently identified PsSiAdV from the critically endangered-orange-bellied parrot, which is also the common ancestor of all avian siadenoviruses within the group, was also selected due to its pressing necessity for immediate actions on disease management (Athukorala et al., 2021). In addition, the extensively researched and highly relevant HAdV was also chosen as a representative pVII model (Benkő et al., 2021; Haruki et al., 2003; Lee et al., 2003; Ostapchuk et al., 2017; Sharma et al., 2017; Wodrich et al., 2006; Zhang and Arcos, 2005). We conducted experiments for these four constructs across different bacterial strains and expression systems, revealing that pVII from each of the four species exhibited distinct preferences for specific bacterial strains and conditions. This highlights the critical significance of meticulously selecting the most suitable protein production system during the preliminary stages. Insoluble proteins present additional challenges to the crystallisation process due to the inherent tendency of protein to aggregate or precipitate and the associated protein refolding procedures (Lieberman et al., 2013; Russo Krauss et al., 2013).

Our study aimed to advance the analysis of the pVII structure. To address the challenges posed by insoluble proteins, we initially explored the soluble segment of pVII. Prior research has highlighted the possibility of recombinant protein VII obstructing the His-Tag in its folded state, rendering it inaccessible to Ni2+ on the affinity column (Sharma et al., 2017). Consistent with this phenomenon, we also observed a higher concentration of target proteins eluted with the flowthrough. Remarkably, the chromatogram revealed a substantial increase in the target protein's yield following treatment of the extracted soluble fraction with RNase and a preliminary incubation before affinity purification. While adenovirus pVII is recognised as a DNA binding protein (Kulanayake and Tikoo, 2021), our study involving RNase unveiled the capacity of the highly cationic pVII to associate with cellular RNA, akin to proteins capable of binding diverse RNA types (Hudson and Ortlund, 2014). Despite achieving a high level of purity, the protein concentrations remained relatively low in soluble fraction, prompting our consideration of examining the proteins within the insoluble fraction.

Purifying inclusion bodies of pVII presents a formidable challenge

due to its highly cationic nature and its tendency to non-specifically bind with other fusion proteins such as TEV and thioredoxin (Sharma et al., 2017). In this study, we engineered constructs incorporating only the TEV site to enable the cleavage of the His-Tag, facilitating the subsequent release of pVII post-purification. To optimise pVII purification conditions, we conducted a preliminary investigation, building upon previous attempts involving a variety of cell lysis, denaturing, and dialysis conditions for both pVII and other insoluble proteins (Haruki et al., 2003; Peternel and Kome, 2010; Sharma et al., 2017; Singh et al., 2015). In line with Peternel and Kome (2010), chemical approaches demonstrated superior efficacy; however, our study employed a combination of chemical and mechanical cell lysis, which proved to be a more efficient approach. In terms of dialysis solution, no significant difference was observed when employing Tris or GST A buffers but effective than water (results not presented) for a successful purification of proteins in substantial quantities. Regrettably, during the dialysis process to remove the denaturing agent urea, pVII displayed a proclivity for easy precipitation. However, interestingly, western blot analysis clearly revealed elevated levels of the target protein in both the precipitate and supernatant fractions collected after dialysis, prompting us to pursue an analytical purification of the solvent portion. This approach led to the successful purification of the target pVII (HAdV pVII purification results are depicted in Fig. 5) with a significantly narrowed peak in the chromatogram, resulting in a higher protein elution yield. Further extended analysis is necessary to determine the functionality of the protein.

In conclusion, this work highlights the importance of continuous refinement and innovation in protein purification techniques, especially for challenging targets like insoluble proteins. Future studies can build upon the strategies and lessons learned from this research, paving the way for advancements in both protein purification methodologies and our understanding of the functional and structural aspects of critical proteins like adenovirus pVII.

CRediT authorship contribution statement

Ajani Athukorala: Conceptualization, Methodology, Investigation, Writing - original draft. **Karla J. Helbig:** Writing - review & editing, Supervision. **Brian P. McSharry:** Writing - review & editing, Supervision. **Jade K. Forwood:** Conceptualization, Methodology, Writing - review & editing, Supervision. **Subir Sarker:** Conceptualization, Methodology, Resources, Writing - review & editing, Supervision, Project administration, Funding acquisition.

Declaration of Competing Interest

The authors declare that they have no known competing financial interests or personal relationships that could have appeared to influence the work reported in this paper.

Acknowledgments

The authors would like to thank La Trobe University (LTU) for the financial support to Ajani Athukorala under the LTU Graduate Research Scholarship and LTU Full Fee Research Scholarship. Subir Sarker is the recipient of an Australian Research Council Discovery Early Career Researcher Award (grant number DE200100367) funded by Australian Government. The Australian Government had no role in study design, data collection and analysis, decision to publish, or preparation of the manuscript.

Appendix A. Supporting information

Supplementary data associated with this article can be found in the online version at doi:10.1016/j.jviromet.2024.114907.

References

Athukorala, A., Donnelly, C.M., Pavan, S., Nematollahzadeh, S., Djossou, V.A., Nath, B., Helbig, K.J., Di Iorio, E., McSharry, B.P., Alvisi, G., Forwood, J.K., Sarker, S., 2024. Structural and functional characterization of siadenovirus core protein VII nuclear localization demonstrates the existence of multiple nuclear transport pathways. J. Gen. Virol. 105 (001928).

Athukorala, A., Forwood, J.K., Phalen, D.N., Sarker, S., 2020. Molecular characterisation of a novel and highly divergent passerine adenovirus 1. Viruses 12.

Athukorala, A., Helbig, K.J., McSharry, B.P., Forwood, J.K., Sarker, S., 2022. Adenoviruses in avian hosts: recent discoveries shed new light on adenovirus diversity and evolution. Viruses 14.

Athukorala, A., Phalen, D.N., Das, A., Helbig, K.J., Forwood, J.K., Sarker, S., 2021. Genomic characterisation of a highly divergent siadenovirus (Psittacine Siadenovirus F) from the critically endangered orange-bellied parrot (Neophema chrysogaster). Viruses 13, 1714.

Avgousti, D.C., Della Fera, A.N., Otter, C.J., Herrmann, C., Pancholi, N.J., Weitzmana, M. D., 2017. pVII Downregulates the DNA damage response. J. Virol. 91, e01089–01017.

Benjin, X., Ling, L., 2020. Developments, applications, and prospects of cryo-electron microscopy. Protein Sci. 29, 872–882.

Benkő, M., Aoki, K., Arnberg, N., Davison, A.J., Echavarría, M., Hess, M., Jones, M.S., Kaján, G.L., Kajon, A.E., Mittal, S.K., Podgorski, I.I., Martín, C.S., Wadell, G., Watanabe, H., B, H., 2021. ICTV virus taxonomy profile: adenoviridae 2021. J. Gen. Virol. 103.

Chen, S., Tian, X., 2018. Vaccine development for human mastadenovirus. J. Thorac. Dis. 10, S2280–S2294.

Dai, X., Wu, L., Sun, R., Zhou, Z.H., Banks, L., 2017. Atomic structures of minor proteins VI and VII in human adenovirus. J. Virol. 91.

Davison, A., Wright, K., Harrach, B., 2000. DNA sequence of frog adenovirus. J. Gen. Virol. 81, 2431–2439.

Gallardo, J., Perez-Illana, M., Martin-Gonzalez, N., San Martin, C., 2021. Adenovirus structure: what is new? Int. J. Mol. Sci. 22.

Harrach, B., Megyeri, A., Papp, T., Ursu, K., Boldogh, S.A., Kajan, G.L., 2022. A screening of wild bird samples enhances our knowledge about the biodiversity of avian adenoviruses. Vet. Res Commun.

Harrach, B., Tarjan, Z.L., Benko, M., 2019. Adenoviruses across the animal kingdom: a walk in the zoo. FEBS Lett. 593, 3660–3673.

Haruki, H., Gyurcsik, B., Okuwaki, M., Nagata, K., 2003. Ternary complex formation between DNA-adenovirus core protein VII and TAF-Ibeta/SET, an acidic molecular chaperone. FEBS Lett. 555, 521–527.

Hindley, C.E., Lawrence, F.J., Matthews, D.A., 2007. A role for transportin in the nuclear import of adenovirus core proteins and DNA. Traffic 8, 1313–1322.

Hudson, W.H., Ortlund, E.A., 2014. The structure, function and evolution of proteins that bind DNA and RNA. Nat. Rev. Mol. Cell Biol. 15, 749–760.

Johnson, J.S., Osheim, Y.N., Xue, Y., Emanuel, M.R., Lewis, P.W., Bankovich, A., Beyer, A.L., Engel, D.A., 2004. Adenovirus protein VII condenses DNA, represses transcription, and associates with transcriptional activator E1A. J. Virol. 78, 6459–6468.

Karamendin, K., Kydyrmanov, A., Fereidouni, S., 2021. High Mortality in Terns and Gulls Associated with Infection with the Novel Gull Adenovirus. J. Wildl. Dis. 57, 662–666.

Karen, K.A., Hearing, P., 2011. Adenovirus core protein VII protects the viral genome from a DNA damage response at early times after infection. J. Virol. 85, 4135–4142.

Kovács, G.M., Davison, A.J., Zakhartchouk, A.N., Harrach, B., 2004. Analysis of the first complete genome sequence of an Old World monkey adenovirus reveals a lineage distinct from the six human adenovirus species. J. Gen. Virol. 85, 2799–2807.

Kulanayake, S., Tikoo, S.K., 2021. Adenovirus core proteins: structure and function. Viruses 13.

Lee, T.W.R., Blair, G.E., Matthews, D.A., 2003. Adenovirus core protein VII contains distinct sequences that mediate targeting to the nucleus and nucleolus, and colocalization with human chromosomes. J. Gen. Virol. 84, 3423–3428.

Lieberman, R.L., Peek, M.E., Watkins, J.D., 2013. Determination of soluble and membrane protein structures by X-ray crystallography. Methods Mol. Biol. 955, 475–493.

Lynch 3rd, J.P., Kajon, A.E., 2016. Adenovirus: epidemiology, global spread of novel serotypes, and advances in treatment and prevention. Semin. Respir. Crit. Care Med. 37, 586–602.

Maclachlan, N.J., Dubovi, E.J., 2017. Chapter 10 - Adenoviridae. In: MacLachlan, N.J., Dubovi, E.J. (Eds.), Fenner's Veterinary Virology, Fifth Edition. Academic Press, Boston, pp. 217–227.

Medkour, H., Amona, I., Akiana, J., Davoust, B., Bitam, I., Levasseur, A., Tall, M.L., Diatta, G., Sokhna, C., Hernandez-Aguilar, R.A., Barciela, A., Gorsane, S., La Scola, B., Raoult, D., Fenollar, F., Mediannikov, O., 2020. Adenovirus infections in african humans and wild non-human primates: great diversity and cross-species transmission. Viruses 12, 657.

Mysiak, M.E., Holthuizen, P.E., van der Vliet, P.C., 2004. The adenovirus priming protein pTP contributes to the kinetics of initiation of DNA replication. Nucleic Acids Res. 32, 3913–3920.

Needle, D.B., Selig, M.K., Jackson, K.A., Delwart, E., Tighe, E., Leib, S.L., Seuberlich, T., Pesavento, P.A., 2019. Fatal bronchopneumonia caused by skunk adenovirus 1 in an African pygmy hedgehog. J. Vet. Diagn. Investig. 31, 103–106.

Nemerow, G.R., Stewart, P.L., Reddy, V.S., 2012. Structure of human adenovirus. Curr. Opin. Virol. 2, 115–121.

Ostapchuk, P., Suomalainen, M., Zheng, Y., Boucke, K., Greber, U.F., Hearing, P., 2017. The adenovirus major core protein VII is dispensable for virion assembly but is essential for lytic infection. PLoS Pathog. 13, e1006455.
Pérez-Vargas, J., Vaughan, R.C., Houser, C., Hastie, K.M., Kao, C.C., Nemerow, G.R., 2014. Isolation and characterization of the DNA and protein binding activities of adenovirus core protein V. J. Virol. 88, 9287–9296.
Peternel, S., Kome, R., 2010. Isolation of biologically active nanomaterial (inclusion bodies) from bacterial cells. Microb. Cell Factor. 9.
Prage, L., Pettersson, U., 1971. Structural proteins of adenoviruses: VII. Purification and properties of an arginine-rich core protein from adenovirus type 2 and type 3. Virology 45, 364–373.
Russo Krauss, I., Merlino, A., Vergara, A., Sica, F., 2013. An overview of biological macromolecule crystallization. Int. J. Mol. Sci. 14, 11643–11691.
San Martín, C., 2012. Latest insights on adenovirus structure and assembly. Viruses 4, 847–877.
Sharma, G., Moria, N., Williams, M., Krishnarjuna, B., Pouton, C.W., 2017. Purification and characterization of adenovirus core protein VII: a histone-like protein that is critical for adenovirus core formation. J. Gennaral Virol. 98, 1785–1794.
Singh, A., Upadhyay, V., Upadhyay, A.K., Singh, S.M., Panda, A.K., 2015. Protein recovery from inclusion bodies of Escherichia coli using mild solubilization process. Microb. Cell Factor. 14, 41.
Syamily, S., Rajasekhar, R., Anoopraj, R., Ravishankar, C., Jishnu, H.P., 2022. Detection and molecular characterisation of canine adenovirus type 1 from a fatal case of infectious canine hepatitis from India. Vet. Rec. Case Rep., e698
Ugai, H., Borovjagin, A.V., Le, L.P., Wang, M., Curiel, D.T., 2007. Thermostability/infectivity defect caused by deletion of the core protein V gene in human adenovirus type 5 is rescued by thermo-selectable mutations in the core protein X precursor. J. Mol. Biol. 366, 1142–1160.
Wodrich, H., Cassany, A., D'Angelo, M.A., Guan, T., Nemerow, G., Gerace, L., 2006. Adenovirus core protein pVII is translocated into the nucleus by multiple import receptor pathways. J. Virol. 80, 9608–9618.
Xue, Y., Johnson, J.S., Ornelles, D.A., Lieberman, J., Engel, D.A., 2005. Adenovirus protein VII functions throughout early phase and interacts with cellular proteins SET and pp32. J. Virol. 79, 2474–2483.
Zhang, W., Arcos, R., 2005. Interaction of the adenovirus major core protein precursor, pVII, with the viral DNA packaging machinery. Virology 334, 194–202.